Mitigation of Chromium Impurity Effects and Degradation in Solid Oxide Fuel Cells: The Roles of Reactive Transport and Thermodynamics

DE-FE0023325

Final Technical Report

Submitted By

Srikanth Gopalan
Department of Mechanical Engineering &
Division of Materials Science and Engineering
Boston University
Boston, MA 02215

Period of Performance:
10/1/2014 to 9/30/2018

Submitted June 2019

BU DUNS #: 049435266

Srikanth Gopalan

ABSTRACT

The principal objectives of this project were to understand the combined role of transport and thermodynamics in chromium poisoning of solid oxide fuel cell (SOFC) cathodes. Specifically, the differences in the chromium poisoning phenomena in predominantly electronic conducting cathodes such as strontium-doped lanthanum manganite (LSM) and mixed conducting cathodes such as strontium-doped lanthanum ferrite (LSF) and lanthanum nickelate (LNO) have been experimentally elucidated. The voltage-current density curves obtained from single cells featuring these cathode materials in the presence of chromium impurity have been analyzed using a suitable electrochemical model. The results clearly show the higher chromium tolerance of LSF and LNO cathodes compared to LSM cathodes. Further, dense protective coatings of copper-manganese spinel oxide applied via electrophoretic deposition (EPD) conformally on ferritic stainless steel current collectors that simulate the interconnection in SOFC stacks have been applied to SOFCs featuring LSM cathodes. Operation over a period of ten days of SOFCs featuring bare and spinel –coated ferritic stainless steel mesh current collectors show that the coatings are highly effective to protect against chromium poisoning.

A. Objectives

The specific objectives of the proposed project are: to understand the individual and combined roles played by reactive transport and thermodynamics in the reaction chemistry of cathodes in the presence of chromium impurities whose origin is the ferritic alloys used as interconnects; to explore, validate, and implement chromium tolerant cathode materials in single cells and short stacks and, to lower the degradation rate due to chromium of baseline cells with LSM cathodes, by using improved cathodes by 50%; and to implement interconnect barrier layers developed previously by Boston University (BU) and demonstrate a 50% improvement in degradation rates compared to baseline interconnects.

B. Scope of the Project

The original scope of the project included:

(a) Baseline estimates and electrochemical modeling of the performance of single cells with various cathode materials with and without exposure to chromium from ferritic stainless steels.

(b) Fabrication and testing of cells with patterned cathodes exposed to chromium impurities from ferritic stainless steels.

(c) TEM and microstructural analysis on both complete solid oxide fuel cells (SOFCs), and on the patterned electrode cathodes will be performed to determine the location and composition of various phases that form in these materials systems.

(d) Developing an understanding of compound formation in the SOFC cathode in the presence of chromium by combining reaction transport phenomena and thermodynamic data from literature.

(e) Fabrication and testing of single cells comprising cathodes with graded compositions. The strategy for compositional grading will be developed based on the results of TEM and microstructural analysis on both complete SOFCs and patterned electrode cells.

(f) Development of interconnect coatings that will act as a barrier layer for Cr evaporation.

(g) Testing of short stacks featuring graded cathode cells and interconnects with barrier layers.

Eventually during the conduct of the project, porous electrodes were chosen over patterned electrodes and the effort to test short stacks was replaced by a greater emphasis on the development of protective coatings and single cells.

C. Tasks and Accomplishments

Task 1 - Project Management, Planning and Reporting

- All required reports have been submitted.

Task 2 - Solid Oxide Fuel Cell Fabrication, Testing and Analysis

Cell Fabrication of Complete SOFCs: In this study, commercially available cell structures (Materials and Systems Research Inc., USA) consisting of a Ni/8YSZ (8 mol% Y_2O_3–92 mol% ZrO_2) anode substrate, a Ni/8YSZ anode interlayer and an 8YSZ electrolyte, were employed. The NiO:YSZ weight ratio was 50:50 in both anode substrate and anode interlayer before cell reduction. The thicknesses of anode substrate, anode interlayer and electrolyte are approximately 750µm, 10µm and 8 µm, respectively. The approximate area of anode (and electrolyte) was 7.3 cm^2. A LSM/8YSZ composite cathode active layer and a LSM cathode current collector layer were applied over the 8YSZ electrolyte by screen printing. Cathode active layer slurry was prepared by mixing $(La_{0.8}Sr_{0.2})_{0.95}MnO_{3-\delta}$ (Fuel Cell Materials, USA) and 8YSZ (Tosoh Corp., Japan) powders in 50:50 wt% and ball milling for 10 hours in alpha-terpineol (Alfa Aesar, USA) with the desired amount of pore former (Carbon lampblack, Fisher Scientific, USA) and binder (V6, Heraeus, USA). Cathode current collector layer slurry was prepared by mixing overnight $(La_{0.8}Sr_{0.2})_{0.95}MnO_{3-\delta}$ powder with the desired amount of pore former (Carbon black, Fisher Scientific, USA) and binder (V6, Heraeus, USA) in alpha-terpineol. Zirconia balls with diameter of 10 mm (Tosoh Corp. Japan) were used as grinding media for preparing the slurries of cathode layers. After screen printing of each layer, the cell structure was sintered at 1200◦C for 2 hours. After sintering, the thicknesses of cathode active layer and cathode current collector layer were approximately 30 µm and 50 µm, respectively. The approximate cathode area was 2 cm^2. Similarly, cells comprising strontium-doped lanthanum iron oxide (LSF) and lanthanum nickelate (LNO) cathodes and featuring a barrier layer of 10 mol% Gd_2O_3-doped ceria (GDC10) were also fabricated and tested.

Cell Testing of Complete SOFCs: The schematic of the cell test-setup is shown in Fig.1 below.

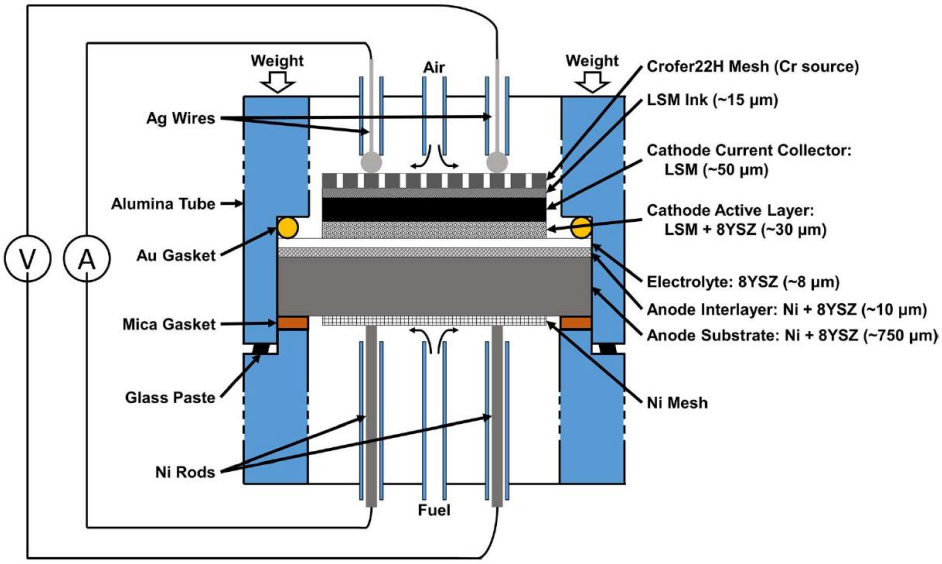

Fig.1: *Schematic of cell testing setup*

Crofer22H (Fe-Cr-Mn alloy) was used as the inter-connect material in this work. Crofer22H mesh with mesh opening of about 0.6 × 0.9 mm and thickness of 0.2 mm, was commercially purchased from Fiaxell S`arl (Switzerland). As part of the cell assem-bly, the Crofer22H mesh was cut into round shape having the same area as the cathode (2 cm^2), and was attached on the cathode with LSM ink (a LSM slurry and polyvinyl butyral mixture) for current collection. A Ni mesh was also pre-attached on the anode with Ni ink (Fuel Cell Materials, USA). Figure 1 shows the schematic of the setup for cell testing. It is comprised of two alumina tubes, with the cell sandwiched between them. Two silver wires with silver beads on the ends were pressed (by spring loading of less than 0.5 kg) on the Crofer22H mesh to serve as current and voltage probes on the cathode side, and two Ni rods were pressed on the Ni mesh to serve as current and voltage probes on the anode side. A gold gasket (Scientific Instru-ment Services, Inc., USA) on the cathode side and a mica gasket (Fuel Cell Materials, USA) on the anode side were compressed by spring loading of approximately 5 kg to obtain gas tightness. In addition, glass paste (Fuel Cell Store, USA) was applied outside the alumina tubes around the mating circumference to ensure a tight seal.

The cells were electrochemically tested at 800°C. In order to sim-ulate low fuel utilization condition, 98% H_2 –2%H_2O was circulated over the anode (obtained by bubbling H_2 through a water bath at ~18◦C). The fuel flow rate was 300 cm^3/min, which provided a flooded fuel condition and negligible fractional fuel utilization. Initially, dry air was circulated over the cathode at a flow rate of 1000 cm^3/min (with gas velocity of approximately 4.8 m/s at 800°C), also providing a flooded condition with negligible fractional oxidant uti-lization. The cells were first operated under open-circuit condition for at least 48 hours so that the cells could equilibrate. Galvanostatic pre-treatment process prior to actual cell testing was not suitable in this experiment because it would cause undesired Cr-related degradation prior to the actual measurements. After the cell performances became stable under open-circuit condition, the initial performances of the cells were characterized by current-voltage (C-V) measurements. After the initial performance measurements, different cathode atmospheres and current conditions were imposed on identical cells (from the same batch). Dry air was obtained by passing compressed air through desiccant, and 10% humidified air was obtained by passing the dry air through a water bubbler maintained at 46°C (the gas tubing for the humidified air was heated to prevent condensation of the water vapor). A Princeton Applied Research PARSTAT 2273 potentiostat and a KEPCO BOP 20-20M power amplifier were used for all electrochemical measurements.

Figure 2 shows the C-V curves and the corresponding power density data of the four cells operated under different cathode atmospheres and current conditions. The ini-tial maximum power densities of these four cells (measured under the same initial dry air and open-circuit condition) were very close (0.45±0.02 $W/^{cm2}$), indicating consistent initial cell performances (see Figure 2 for 0 h test results). However, after different cell operating conditions were imposed, different degradation behaviors of cell performances were observed from the C-V curves, and they can be described as follows:

(a) Cell A, which was operated under open-circuit condition with dry air flowing over the cathode, had no observable performance degradation (see Figure 2a). The initial maximum power density of this cell was 0.43 W/cm^2, and that after 120 hours was 0.44 W/cm^2. The slight improvement of cell performance may be associated with the cell

break-in, since no pre-treatment was performed.

(b) Cell B was also tested in a dry air cathode atmosphere. Unlike Cell A, Cell B was operated under a constant cathodic current density of 0.5 A/cm^2 after the initial performance was measured. Significant degradation of the cell performance was observed (see Figure 2b). The maximum power densities decreased as follows: 0.44 W/cm^2 (0 h), 0.32 W/cm^2 (24 h), 0.28 W/cm^2 (48 h), 0.27 W/cm^2 (72 h), 0.26 W/cm^2 (96 h) and 0.25 W/cm^2 (120 h). The cell performance degraded rapidly during the first 24 hours of the imposed galvanostatic condition. After the rapid initial degradation, the rate of degradation decreased. In total, the maximum power density of Cell B decreased by approximately 43% in 120 hours.

(c) Cell C was operated under open-circuit condition with 10% humidified air over the cathode. Similar to Cell A, no performance degradation of Cell C was observed (see Figure 2c). The maxi-mum power density of this cell increased from 0.46 W/cm^2 at 0 hour to 0.47 W/cm^2 at 120 hours (reason same as in (a)).

(d) Cell D was tested in an extreme condition: under a constant cathodic current density of 0.5 A/cm^2 with 10% humidified air over the cathode. A dramatic degradation of cell performance was observed in the first 24 hours, followed by a steady deterioration. The maximum power densities decreased as follows: 0.47 W/cm^2 (0 h), 0.20 W/cm^2 (24 h), 0.17 W/cm^2 (48 h), 0.16 W/cm^2 (72 h), 0.14 W/cm^2 (96 h) and 0.12 W/cm^2 (120 h). Overall, the maximum power density of Cell D decreased by approximately 74% in 120 hours.

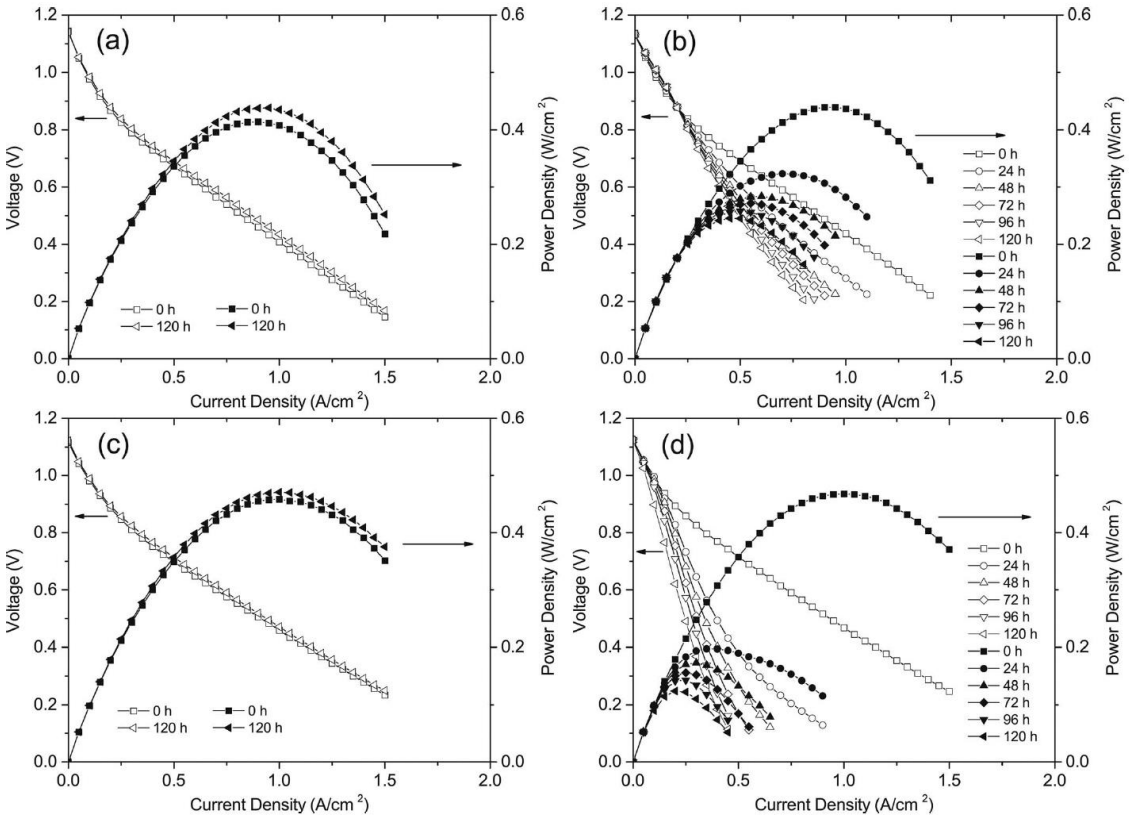

Fig.2: *Electrochemical test results of (a) cell A, (b) cell B, (c) cell C, and (d) cell D*

Cross-sectional SEM images and SEM spectra of the tested cells are shown in Figure 3.

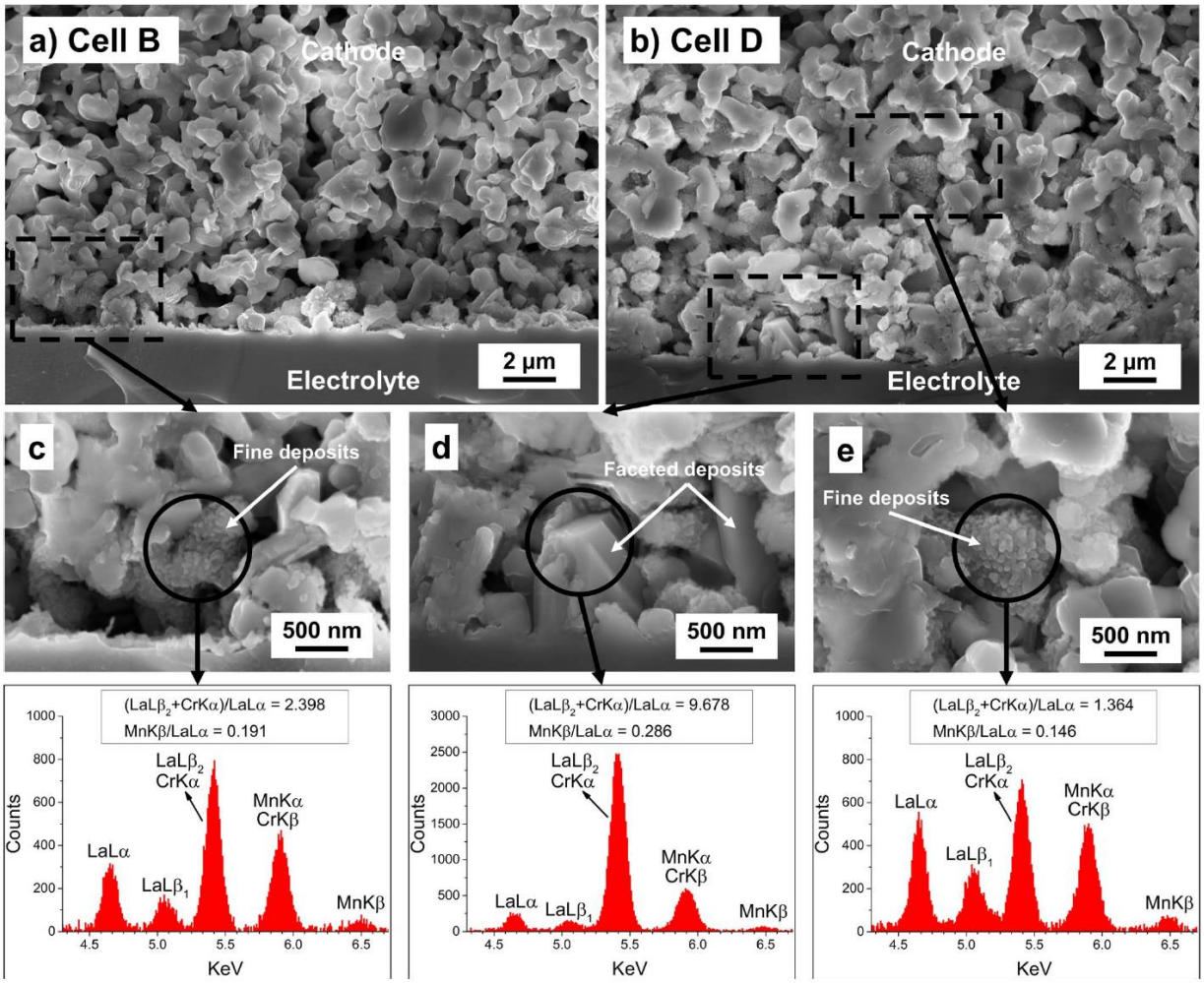

Fig. 3: *SEM micrographs of cathode cross sections in fractured cells and the corresponding EDX analyses in (a, c) Cell B: tested with dry air under 0.5 A/cm^2 cathodic current density, and (b, d, e) Cell D: tested with 10% humidified air under 0.5 A/cm^2 cathodic current density.*

It can be seen from the SEM-EDX results that the deposits of Cr-containing product phases are worsened by high current density combined with the presence of humidity. The measured chromium enrichment in the cathode is plotted as a function of position within the cathode in Figure 4. It is seen clearly that the most serious chromium poisoning occurs when both high current conditions and humidity are simultaneously present in the cathode. More details can be found in reference [1].

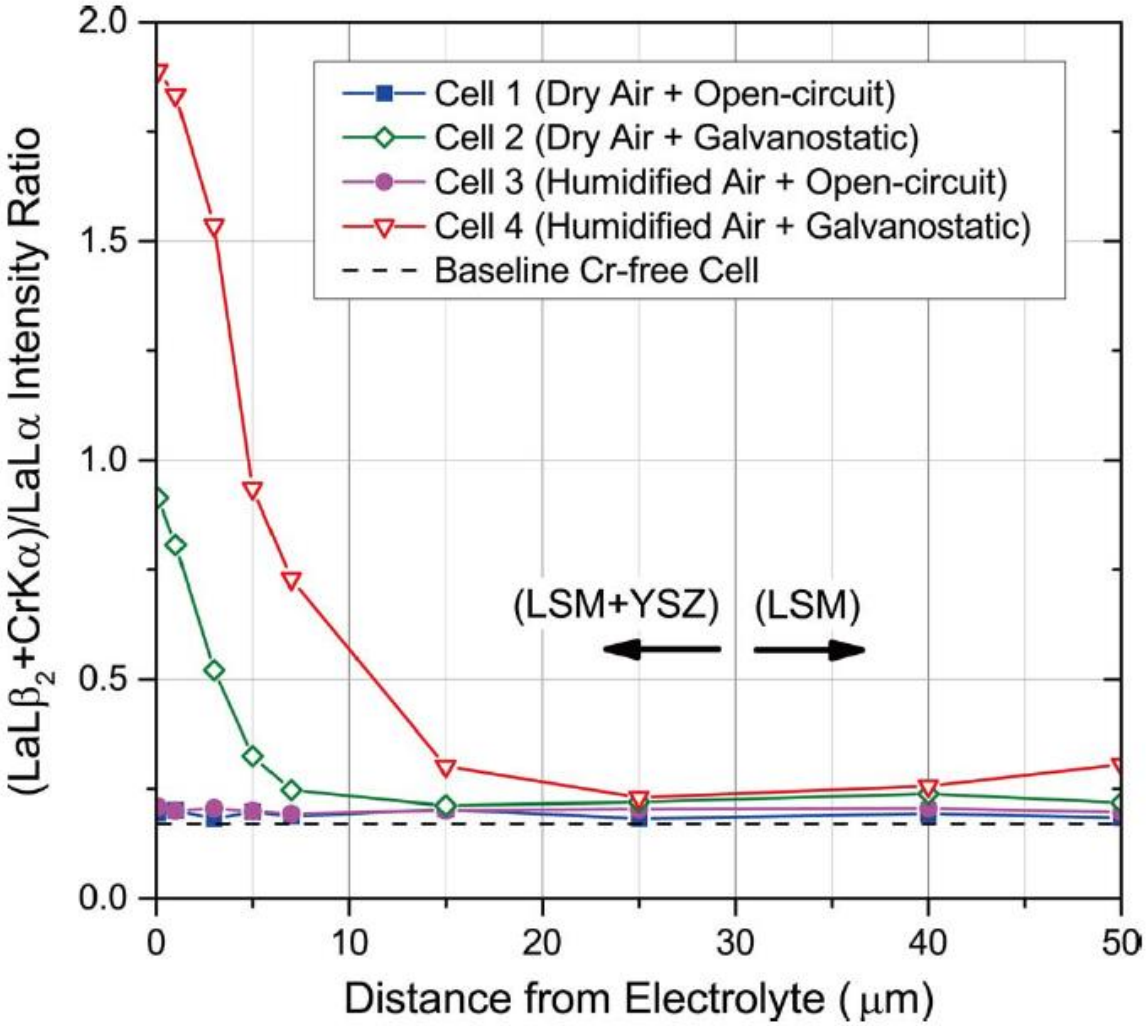

Fig.4: *(LaLβ2+CrKα)/LaLα intensity ratios measured at different cathode thickness positions, relative to the electrolytes of four tested cells; cell 4 with humidified air and a galvanostatic current of 0.5 A/cm^2 shows the highest levels of chromium poisoning effects*

LSF and LNO cells were also similarly tested. The performance of the LSF cells at 0.5 A/cm^2 current density is compared with that of the LSM cells in Figure 5. It is clear that over a period of 120 h, the degradation in LSF cathodes is not evident, unlike the LSM cathodes which show significant degradation over the 120 h period. Microstructural characterization of the tested LSF cathodes show that Cr-containing deposits also form in the cells featuring LSF cathodes. However, the chromium poisoning effects are not as significant as in the LSM cells. In particular, the formation of Sr-Cr-O compounds are seen at the LSF-air boundary and only Cr-O compounds at the electrolyte-LSF cathode interface. As in the case of LSM, these effects are more prevalent in cells tested under a constant current of 0.5 A/cm^2 in the presence of humidity. While the LSF cells did not exhibit degradation over the 120 h period when tested in the presence of humidity and current, it is likely that they will show degradation when tested for extended periods. In fact the LSF cells show a modest improvement as seen in Fig. 6 when tested under humidity and current, whereas they show a decline when only tested under humidity at OCV. We can explain this anomalous behavior by considering cell electrochemical conditioning (which improves cell

performance under current) and chromium poisoning (which degrades performance) as two simultaneous competing effects on the cell performance. Over a period of 120 h, the cell electrochemical conditioning dominates the chromium poisoning effects. However, with the passage of time, this may not continue to be true and the cell may eventually start degrading due to chromium poisoning. Longer term test data to be obtained in future projects will be necessary to confirm this. If this were to occur, other means to combat chromium poisoning such as protective coatings and/or chromium gettering will have to be resorted to.

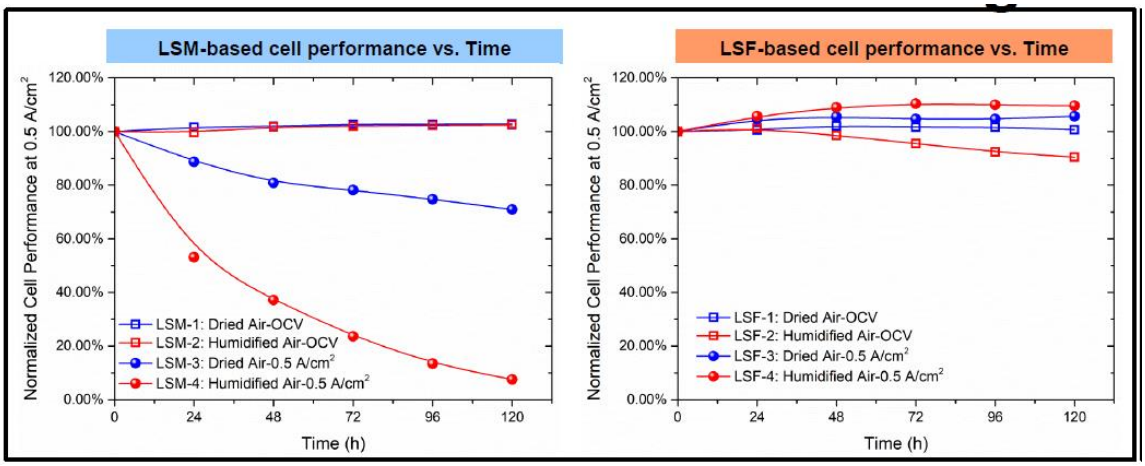

Fig.5*: Left Panel: Degradation behavior of SOFCs with LSM cathodes in contact with ferritic stainless steel current collector while the cells were maintained at OCV in dry air and humidified air and under an operating current density of 0.5 A/cm². Right Panel: Degradation behavior of SOFCs with LSF cathode under the same conditions*

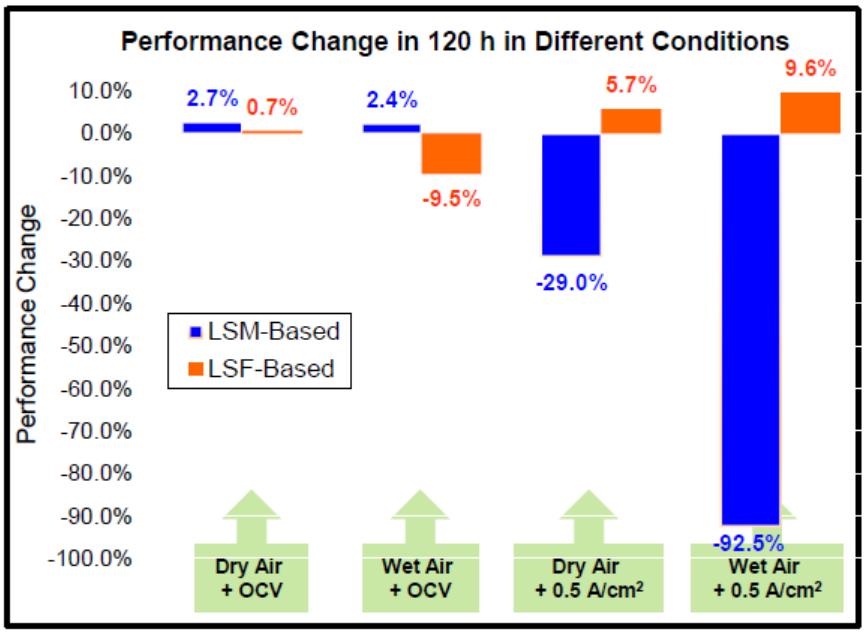

Fig.6: *Summary of performance changes for LSM and LSF cathode cells*

Test results on LNO based cathodes were similar to LSF cathodes in that the resistance to chromium poisoning was greater than LSM cathodes [8].

Task 3 - Patterned Electrode Cell Fabrication, Testing and Analysis

The original goal of this task was to fabricate model patterned electrode and analyze chromium deposition on such model electrodes to get a fundamental understanding of the chromium deposition parameters. The impetus for this task was based on our prior work on patterned electrodes [6,7]. However, during the performance of this project, this proved to be difficult to accomplish primarily due to a shift in the priorities of the Environmental Molecular Sciences Lab (EMSL) at PNNL where much of the patterned electrode fabrication in earlier work was performed. The EMSL lab in recent years has moved away from supporting work in solid state electrochemistry in favor of supporting life sciences. Thus, this task was dropped and a greater emphasis was instead placed on Tasks 2 and 4.

Task 4 – Development of Protective Coatings

Under this task, protective conformal coatings CuMn spinel ($CuMn_{1.8}O_4$) synthesized using the glycine nitrate process family have been deposited and tested on single cells comprising LSM cathodes using electrophoretic deposition (EPD). The interconnect substrates that were coated in this study were 20 mm × 20 mm × 0.1 mm Crofer 22 APU plates (Fuelcellmaterials, Lewis Center, OH) and 2 cm^2 discs of Crofer 22 H mesh (Fiaxell SOFC Technologies, Switzerland). The metallic interconnect substrates were used as the cathode with the anode being a 60 mm × 50 mm Cu plate. The EPD solution consisted of an ethanol and acetone mixture (25:75 vol%, re-spectively) containing the spinel powders (9 mg ml^{-1}) and I2 (1.09 mg ml^{-1}). A constant voltage of 20 V was applied for 10 min. The as-deposited coatings were porous, and had to be subjected to further densification processing. The samples were subjected to a re-duction anneal for 24 h at 1000 °C in forming gas (2% H2 and balance Ar), and then annealed in air at 850 °C for 100 h. The coated samples after the densification processing will be referred hereon as as processed samples. It should be noted that previous densification processing for a different Cu-Mn spinel ($Cu_{1.3}Mn_{1.7}O_4$) coating included mechanical steps consisting of two separate uniaxial pressings [5], which will not work on mesh samples. In this study, the mechanical steps were eliminated by increasing the temperature and time of the reduction. Conformal coatings on ferritic stainless steels have been obtained using this procedure.

Micrographs of the conformal coatings are shown in Fig.7. Results of cells tested at a fixed current density of 0.5 A/cm^2 are shown in Fig.8. It is clear that cells featuring the protective coating perform significantly better over a 10-day period than uncoated cells.

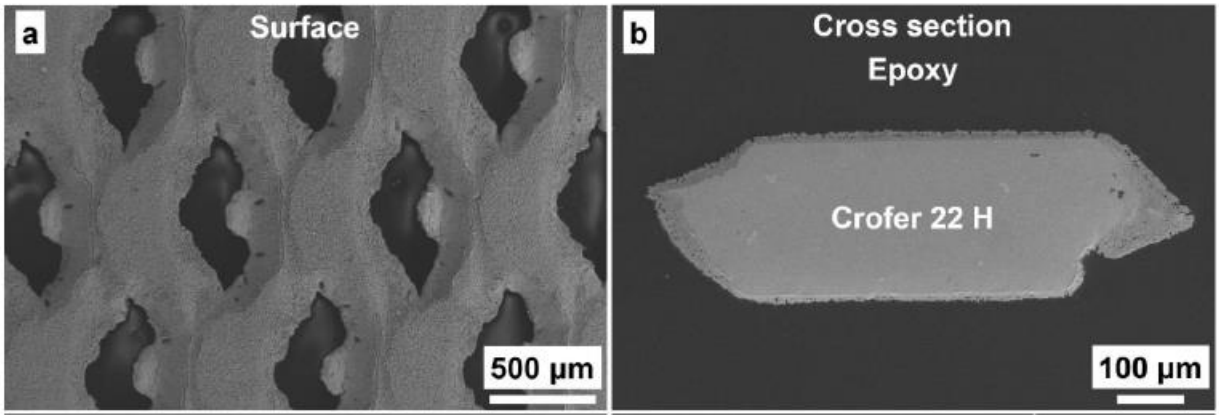

Fig.7: *CuMn spinel deposited over a stainless mesh conformally, using an electrophoretic deposition (EPD) process*

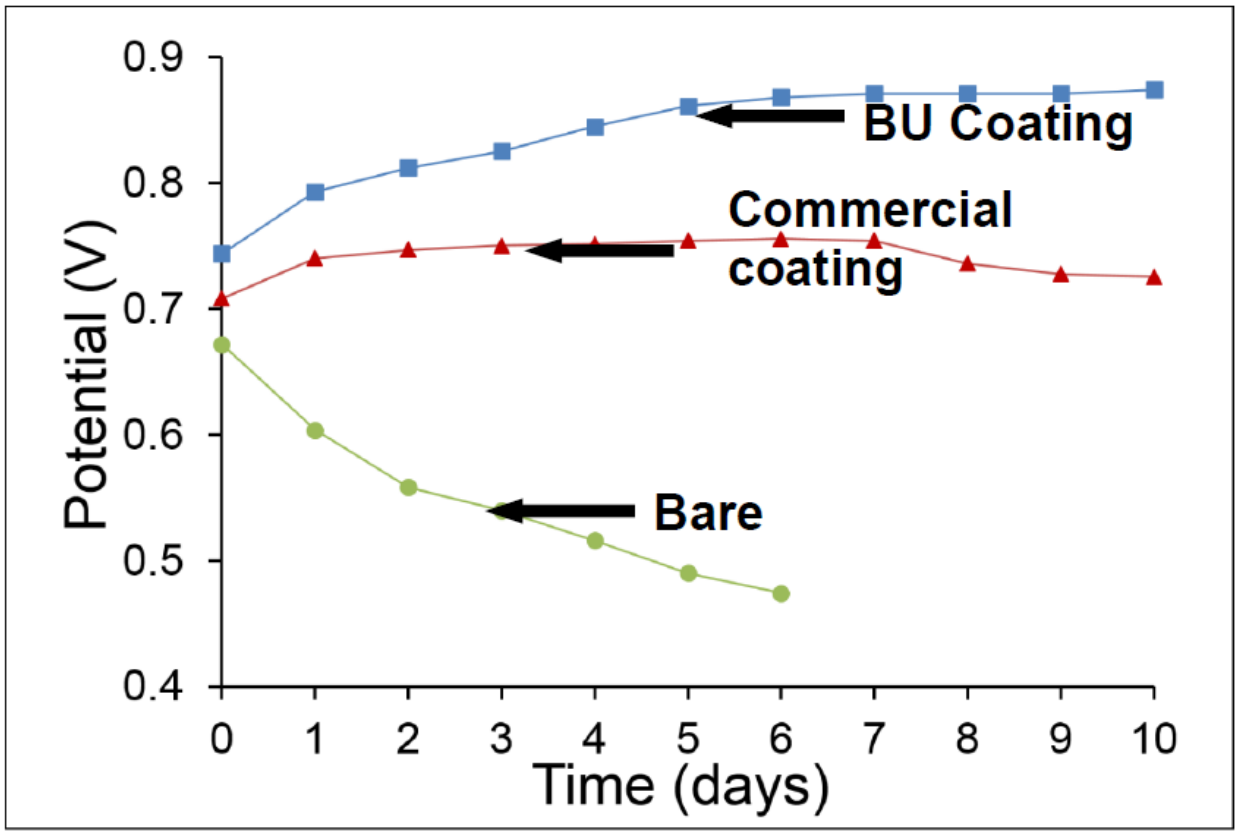

Fig.8: *Voltage versus time of cells at 0.5 A/cm^2 featuring LSM cathode in contact with stainless steel meshes featuring a bare mesh, a mesh with a commercial protective coating, and a cell with a CuMn spinel coating developed in this project by the BU team*

More details can be found in our archival journal publications [3-5].

Task 5 - Numerical Modeling of Chromium Reactive Transport in the Cathode

An electrochemical model has been applied to analyze the voltage-current density data with and without the presence of chromium. The voltage-current density equation used to model the experimental data is given below:

$$V_{cell}(i) = V_o - iR_i - \frac{2RT}{F}\ln\left\{\frac{1}{2}\left[\left(\frac{i}{i_{o,c}}\right)+\sqrt{\left(\frac{i}{i_{o,c}}\right)^2+4}\right]\right\} + \frac{RT}{2F}\ln\left(1-\frac{i}{i_{as}}\right) - \frac{RT}{2F}\left(1+\frac{p^o_{H_2}\,i}{p^o_{H_2O}\,i_{as}}\right) + \frac{RT}{4F}\ln\left(1-\frac{i}{i_{cs}}\right) \quad - \quad (1)$$

The first term on the right hand side (RHS) is the open circuit voltage, the second term is the activation polarization, assumed in this work to occur entirely at the cathode, and the third and fourth terms together are the anode concentration polarization terms, and the last term is the cathode concentration polarization term. This model has allowed us to separate the polarization components and related them to the chromium poisoning effects and the efficacy of the protective coatings in reducing chromium poisoning.

Table I. *Curve fitting results of Cell B and Cell D before and after 24 hours of 0.5 A/cm2 cathodic current.*

	Cell B		Cell D	
Fitting Parameters	0 hour	24 hours	0 hour	24 hours
R_i ($Ohm \cdot cm^2$)	0.169	0.127	0.112	0.104
$i_{o,c}$ (A/cm^2)	0.146	0.066	0.124	0.024
i_{as} (A/cm^2)	2.210	2.210	2.695	2.695
i_{cs} (A/cm^2)	1.760	1.505	1.970	1.078

In particular, Table I shows the results of galvanostatic testing of a cell in dry air (cell B) and and galvanostatic testing in humidified air (cell D) of an LSM cathode cell. The effects on the cathode exchange current density ($i_{o,c}$) and the cathode concentration polarization, i.e. cathode limiting current density, i_{cs} are both clearly seen. After 24 h of testing both of these parameters decrease significiantly; the former due to loss of TPBs and the attendant decrease in exchange current density and the latter due to deposition of Cr-containing products within the cathode and their aggregation leading to a lower cathode limiting current density. However, the former is a more significant effect.

More details can be found in our archival journal publications [1,2].

Task 6 - Testing and Validation of Chromium Tolerant Graded Cathodes Using Single Cell and Short Stack Tests

The initial goal of this task was to validate the chromium tolerant cathodes using single cell and short stack tests. Some of the goals under this task were accomplished in tasks 2 and 4. However,

as we expanded the work to obtain conformal coatings of spinels on mesh interconnections, we were running out of funding for the last graduate student in the project. We then approached Fuel Cell Energy (FCE) who was the original subcontractor on the project. In consultation with DOE, we decided to redirect the funding under this task (which was originally to be performed at FCE) into tasks 2 and 4 where we had demonstrated excellent initial success. As can be seen from the results in task 4, the redirection of funding was more than justified.

D. Key Accomplishments

1) Chromium poisoning effects in LSM cathode has been studied in detailed and the mechanisms of poisoning including the role of current density and humidity have been understood.
2) LSF and LNO cathodes have been tested for resistance towards chromium poisoning. Over a limited period of testing (120 h), both cathodes show no chromium poisoning effects.
3) Conformal CuMn spinel coatings have been deposited on ferritic stainless steel interconnect meshes. The coated mesh shows excellent chromium transport resistance as evidenced by cell tests featuring LSM cathodes over a ten day period.

E. References

1) R. Wang, U.B Pal, S. Gopalan, S. N. Basu, "Chromium poisoning effects on performance of (La, Sr) MnO3-based cathode in anode-supported solid oxide fuel cells," *J.Electrochem.Soc.,* 164 (7) F740-F747 (2017)

2) R. Wang, M.Würth, U. B Pal, S. Gopalan, S N Basu, "Roles of humidity and cathodic current in chromium poisoning of Sr-doped LaMnO3-based cathodes in solid oxide fuel cells," *J Power Sources,* 360 (31) 87-97 (2017)

3) Z Sun, R Wang, A Y Nikiforov, S Gopalan, U B Pal, S N Basu, "CuMn1. 8O4 protective coatings on metallic interconnects for prevention of Cr-poisoning in solid oxide fuel cells," *J Power Sources*, 378 (28) 125-133 (2018)

4) Z Sun, S Gopalan, U B Pal, S N Basu, "Electrophoretically Deposited Copper Manganese Spinel Coatings for Prevention of Chromium Poisoning in Solid Oxide Fuel Cells," *Energy Technology,* 265-272 (2019)

5) Z Sun S Gopalan U B.Pal, S N.Basu, "Cu1.3Mn1.7O4 spinel coatings deposited by electrophoretic deposition on Crofer 22 APU substrates for solid oxide fuel cell applications," *Surf. Coatings.Tech.,* 323, 49-57 (2017)

6) L J Miara, J N Davis, S N Basu, U B Pal, S Gopalan, "Application of a State-Space Model to Patterned Cathodes of (La0. 87Ca0. 13) 0.95 MnO3," *J.Electrochem.Soc.,* 158 (12) B1523-B1531 (2011)

7) L J Miara, J N Davis, S N Basu, U B Pal, S Gopalan, "2D Numerical Model for Identification of Oxygen Reduction Reaction Mechanisms in Patterned Cathodes of

La0.6Sr0.4Co0.2Fe0.8O3-δ," *J.Electrochem.Soc.*, 159 (8) F419-F425 (2012)

8) Y Gong, R Wang, J Banner, S N. Basu, U B. Pal, S Gopalan, "Improved Tolerance of Lanthanum Nickelate (La2NiO4+δ) Cathodes to Chromium Poisoning Under Current Load in Solid Oxide Fuel Cells (*Submitted to JOM; In Review*)